# CCVD synthesis of carbon nanotubes from (Mg,Co,Mo)O catalysts: influence of the proportions of cobalt and molybdenum

**Emmanuel Flahaut,* Alain Peigney, Wolfgang S. Bacsa, Revathi R. Bacsa and Christophe Laurent**

*CIRIMAT UMR CNRS 5085/LCMIE, Centre Interuniversitaire de Recherche et d'Ingénierie des Matériaux, Université Paul-Sabatier, 31062 Toulouse Cedex 4, France. E-mail: flahaut@chimie.ups-tlse.fr; Fax: +33-5 61 55 61 63; Tel: +33-5 61 55 69 70*

Carbon nanotubes have been synthesised by catalytic chemical vapour deposition of a $H_2$–$CH_4$ mixture (18 mol% $CH_4$) over (Mg,Co,Mo)O catalysts. The total amount of cobalt and molybdenum has been kept constant at 1 cat% and the proportion of molybdenum with respect to cobalt has been varied from $x$(Mo) = 0.25–1.0. This variation has important effects on both the yield and the nature (number of walls, straight walls or bamboo-like structures) of the carbon nanotubes. It also has an influence on the purity of the samples (amount of encapsulated metal particles, presence or not of amorphous carbon deposits). For $x = 0.25$, the nanotubes were mainly double- and triple-walled (inner diameter less than 3 nm); samples prepared from catalysts with higher molybdenum ratios contained larger multi-walled carbon nanotubes (inner diameter up to 9 nm), having up to 13 concentric walls. It is proposed that different growth mechanisms may occur depending on the initial composition of the catalyst.

## Introduction

Catalytic chemical vapour deposition (CCVD) is known to be a very flexible method for the synthesis of carbon nanotubes (CNTs). It has been used[1] since 1996 for the production of single-walled CNTs (SWNTs) but was even earlier known to produce multi-walled CNTs (MWNTs). The physical properties of CNTs tend to be more and more similar to those of graphite with the increase in the number of walls. Double-walled CNTs (DWNTs) are at the frontier between SWNTs and the other MWNTs. Double-walled CNTs (DWNTs) may show a better integrability into materials than SWNTs, because of the possibility of modifying their outer wall without disturbing the inner one. This is expected to provide, for example, a better interface when these CNTs are included into composite materials, while preserving the mechanical and electrical properties of the inner tube. For these reasons, DWNTs may prove to be ideal candidates for applications in composite materials. Recent developments of the functionalisation of CNTs have proved the feasibility of this approach. The formation of the CNTs by CCVD routes occurs through the catalytic decomposition of a carbonaceous gas (CO or a hydrocarbon) on nanometric metal particles. The addition of molybdenum to transition metals such as iron and cobalt is known to increase the yield in CNTs but the role it plays in the selectivity towards the number of walls of the CNTs is still in debate. On the one hand for example, Resasco and co-workers[2] used Co–Mo mixtures supported over $SiO_2$ and CO as the carbon source and reported that there was a clear synergistic effect of the mixture compared to the pure metals. They indicated that molybdenum alone was not catalysing the growth of any SWNT (although Dai *et al.*[1] obtained SWNTs in similar conditions, at higher temperature) and that increasing the ratio of molybdenum was favourable. On the other hand, Tang *et al.*,[3] using a mixture of $H_2$ and $CH_4$, reported that only a small ratio of molybdenum within the Co–Mo mixture had a positive effect for the growth of SWNTs.

## Experimental

### Synthesis of carbon nanotubes

The starting oxides were prepared by the combustion route.[4] The formula of the desired combustion products[5] is written as $Mg_{0.99}(Co_{1-x}Mo_x)_{0.01}O$ (with $x$ = 0.25, 0.33, 0.50, 0.67 and 1.0), although these oxides are definitely not solid solutions because the Mo ions do not enter the rock-salt lattice of MgO. $Mg(NO_3)_2{\cdot}6H_2O$ and $Co(NO_3)_2{\cdot}6H_2O$ were dissolved in deionised water together with the required amount of $(NH_4)_6Mo_7O_{24}{\cdot}4H_2O$ as well as urea. Urea was used as the fuel in the combustion process, using three times the so-called stoichiometric ratio.[4] The Pyrex dish containing the solution was placed in a furnace preheated at 550 °C. The solution immediately started to boil and underwent dehydration. The resulting paste frothed and then blazed. A white flame occurred with the production of a rather light material which swelled to the capacity of the Pyrex dish. The total combustion process was over in less than 5 min. The combustion product will be referred as the starting oxide.

For each experiment, 1.5 g of the starting oxide was reduced in a $H_2$–$CH_4$ mixture[5] (18 mol% $CH_4$, heating and cooling rates 5 °C $min^{-1}$, maximum temperature 1000 °C, no dwell). The selective reduction of the starting oxide leads to the formation of nanometric metal particles which immediately catalyse the decomposition of $CH_4$ and are thus progressively loaded with carbon atoms (activation of the nanoparticles). The carbon concentration in the nanoparticles then increases until the solubility limit is reached, followed by the nucleation and growth of a single CNT on each activated metal particle. This resulted in a CNT-containing composite powder with a very homogeneous dispersion of the CNTs around the oxide grains.[5,6] The CNT-containing composite powder was then soaked in an aqueous HCl solution in order to separate the CNTs by dissolving all the remaining oxide material, as well as unprotected metal particles.[5] Unlike nitric acid or other oxidising acids, HCl does not damage the CNTs (no opening of the CNTs, no oxidation of the tips and defects which may be

present on the outer sidewalls). The acidic suspensions were filtered on 0.45 μm pore size cellulose nitrate membranes (Whatman) and washed with deionised water until neutrality. The resulting samples, denoted extracted CNTs, were then dried overnight in air at 80 °C.

### Characterization

X-Ray diffraction (XRD) patterns were obtained using Cu-Kα radiation ($\lambda = 0.15418$ nm). The CNT-containing composite powders were studied using FEG scanning electron microscopy (FEGSEM, Hitachi S4500, operated at 5 kV). Extracted CNTs were observed both by transmission electron microscopy (JEOL 200CX, operated at 120 kV) and by high-resolution transmission electron microscopy (HRTEM, JEOL 2010, operated at 120 kV). The carbon content was determined by flash combustion with an accuracy of $\pm 2\%$. Flash combustion is based on the complete and instantaneous oxidation of the sample; carbon is oxidized into $CO_2$ which is detected by a thermal conductivity detector, giving an output signal proportional to the concentration in the sample. The carbon content is denoted $C_n$ for the CNT-containing composite powders and $C_e$ for the corresponding extracted CNTs samples. The specific surface area of the samples (starting oxides, CNT-containing composite powders and corresponding extracted CNTs) were measured by the BET method using $N_2$ adsorption at liquid-$N_2$ temperature in a Micromeritics FlowSorb II 2300 apparatus. Raman spectra were recorded using a micro-Raman spectrometer (Model XY, Dilor) with back-scattering geometry and at $\lambda = 488$ nm (3–5 mW). The samples were placed on a microscope glass slide.

## Results

X-Ray diffraction (XRD) patterns of the different starting oxides did not reveal any significant difference and only the peaks corresponding to the MgO rock-salt lattice could be observed. Previous work revealed that Co ions are in solid solution in MgO[5] but this is very unlikely for Mo ions. We suppose that molybdenum is present as an $MoO_x$ oxide but the amount is so low (and the particles are probably very small) that it is not possible to detect any trace in the starting oxides by XRD analysis. The BET specific surface area of the

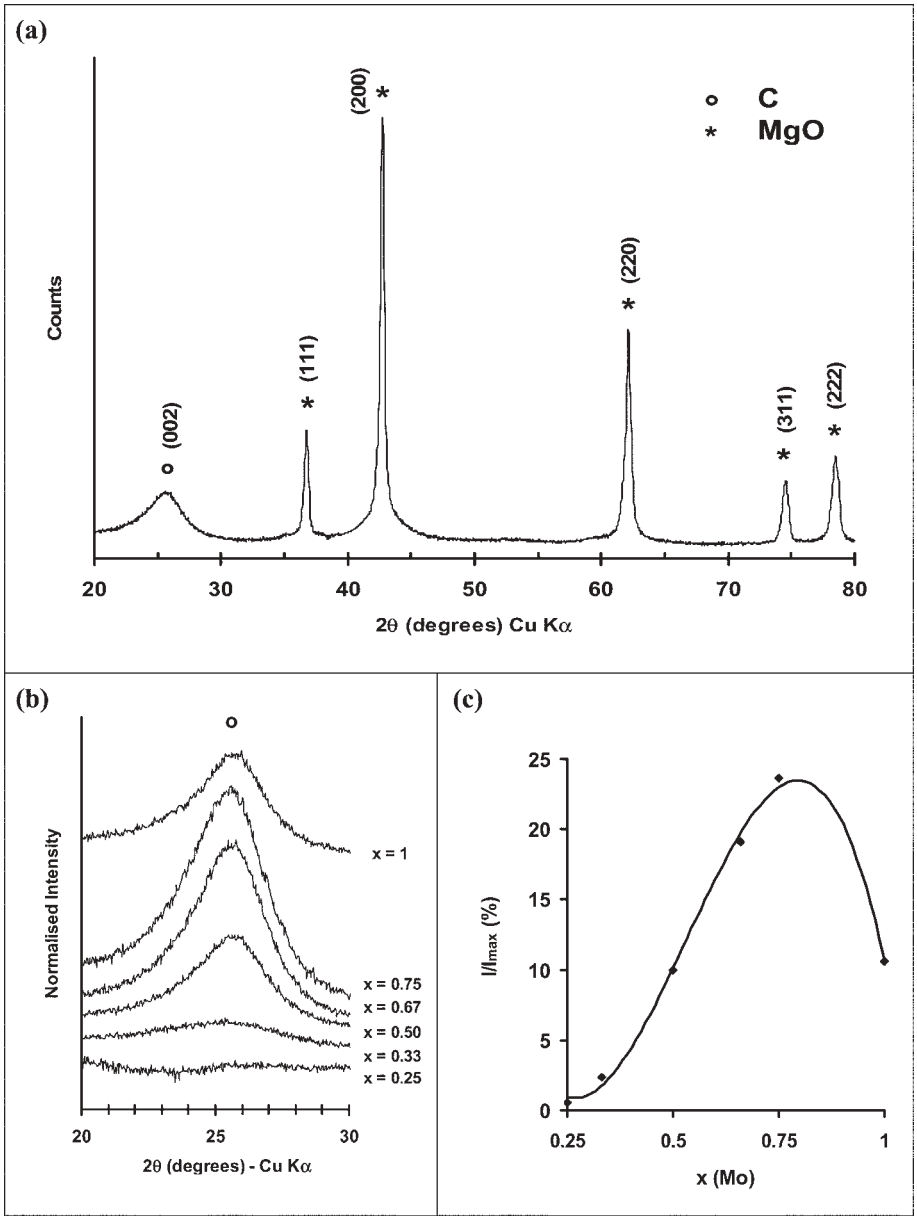


**Fig. 1** (a) Representative XRD pattern of the CNT-containing composite powder prepared from $Mg_{0.99}(Co_{1-x}Mo_x)_{0.01}O$ starting oxide ($x = 0.50$). (b) XRD pattern of the carbon (002) peak of the CNT-containing composite powders ($0.25 \leqslant x \leqslant 1$). (c) Normalised intensity of the (002) peak of the CNT-containing composite powders ($0.25 \leqslant x \leqslant 1$): $I_{(002\text{-C})}/I_{(200\text{-MgO})}$.

starting oxides, $S_{so}$, ranges from 8 to 19 $m^2\ g^{-1}$, with no correlation with the proportion of molybdenum.

XRD patterns of the CNT-containing composite powders (a representative example for $x = 0.50$ is shown in Fig. 1(a)) were very similar to those of the starting oxide, apart from a broad peak around $2\theta = 25.8°$, corresponding to the (002) reflection of graphitic carbon (Fig. 1(b)). The relative intensity of this peak (compared to the intensity of the MgO (200) reflection) increased almost linearly for $x$ ranging from 0.25 to 0.75 and then decreased for $x = 1$ (Fig. 1(b), (c)). The carbon content in the CNT-containing composite powders, $C_n$, increased between $x = 0.33$ and $x = 0.75$ (from almost 10.5 wt% to 38.4 wt%) and then decreased to 20.8 wt% for $x = 1$ (Fig. 2(a)). The presence of CNTs after the CCVD step leads to an increase in the specific surface area[6,7] between $S_{so}$ and $S_r$. Similarly to $C_n$, the specific surface area of the CNT-containing composite powder, $S_r$, increased between $x = 0.33$ and $x = 0.75$ (from almost 50 to 105 $m^2\ g^{-1}$) and then decreased to 66 $m^2\ g^{-1}$ for $x = 1$ (Fig. 2(b)). The observation of the CNT-containing composite powders by FEG-SEM has brought to light important morphological modifications with the increase in the molybdenum ratio. For $x < 0.5$, the FEG-SEM shows typical images of CNTs (Fig. 3(a)), with numerous bundles of CNTs branching extensively all around the oxide grains. From $x = 0.5$, the formation of threads (looking like hair locks) is clearly visible (Fig. 3(b)). These threads seem to emerge from oxide grains (Fig. 3(c)) and are very different from the typically observed bundles of CNTs. The latter generally show a high degree of organisation; on the contrary, the threads do not look organised and the CNTs which compose them are gathered more or less randomly. The filaments composing the threads seem to grow thicker and thicker as $x$(Mo) increases, up to around 30 nm in diameter for $x = 0.75$ (Fig. 3(d)).

XRD analysis of the extracted CNTs revealed the progressive appearance of peaks corresponding to molybdenum carbides (Fig. 4). It seems that different carbides are formed in different proportion depending on the molybdenum ratio in the starting oxide. The presence of fcc-Co in the extracted CNTs could not be detected from the XRD data, and these samples exhibited no obvious magnetic properties (not attracted by a strong permanent magnet). The peak corresponding to graphitic carbon seemed to be superposed to another peak at a slightly lower angle. The origin of this peak has not yet been identified (although it may correspond to a molybdenum carbide), but its relative intensity compared to the (002) reflection of graphitic carbon seems to lower with increasing the molybdenum ratio. The evolution of the carbon content in the extracted CNTs samples ($C_e$) was similar to that of $C_n$ in the corresponding CNT-containing composite powders; it increased between $x = 0.33$ and $x = 0.75$ (from almost 92.4 wt% to 93.6 wt%–which corresponds to 98.6 at% of carbon) and then decreased to 89.5 wt% for $x = 1$ (Fig. 2(c)). These values are very high for CNTs samples which have only been exposed to a mild acidic treatment, aimed at only eliminating the substrate rather than being a strong purification process. The specific surface area of the extracted CNTs samples, $S_e$ (Fig. 2(d)), decreased from 803 $m^2\ g^{-1}$ ($x = 0.25$) to about 270 $m^2\ g^{-1}$ with the increase in the molybdenum ratio (from $x = 0.25$ to 0.66) before slightly increasing for $x = 1$ (330 $m^2\ g^{-1}$). The decrease of the specific surface area could be attributed either to an increase in the mean number of walls of the CNTs or to a bundling effect,[7] or to both.

The Raman spectra of the extracted CNTs are compared in Fig. 5. The increase in $I_{D/G}$, the ratio between the intensity of the D band (1350 $cm^{-1}$) and the G band (around 1570 $cm^{-1}$), is clear but not linear with the increase in the molybdenum ratio (Fig. 6). An increasing $I_{D/G}$ value corresponds to an increased proportion of $sp^3$-like carbon, which is generally attributed to the presence of more structural defects. The D band frequency and linewidth does not depend on $x$(Mo). The G band could in most cases be fitted by a combination of two Lorentzian-shape curves (around 1555 and 1575 $cm^{-1}$, respectively) but a third one (centred around 1604 $cm^{-1}$) was necessary for $x \geqslant 0.50$. The vanishing of the radial breathing mode (RBM) signals of

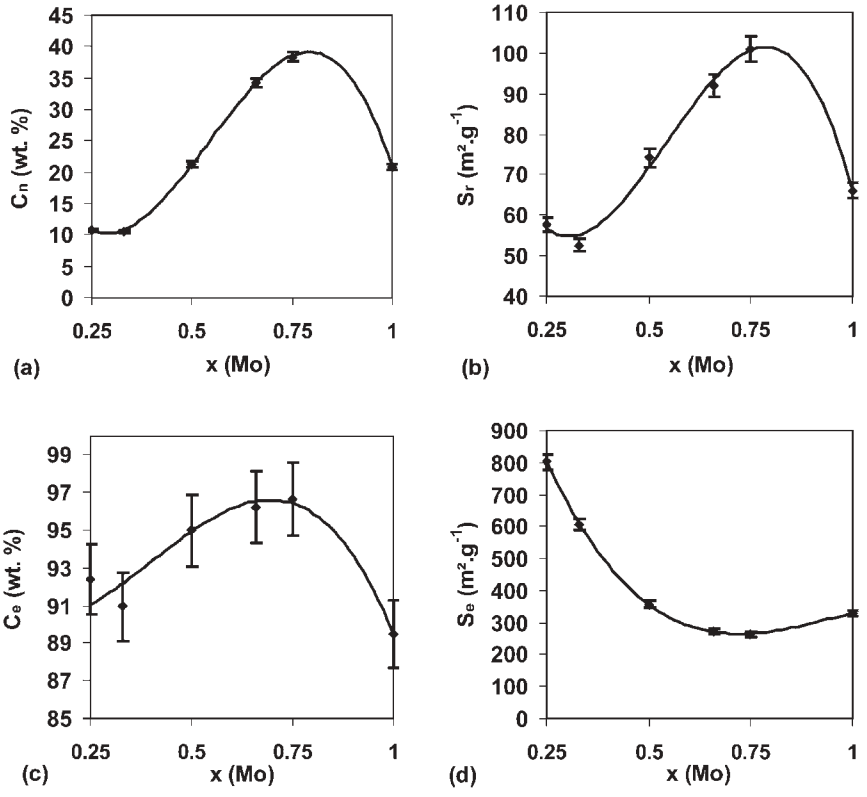


**Fig. 2** Variation of the macroscopic characterisation parameters with the molybdenum ratio in the CNT-containing composite powders: (a) carbon content $C_n$ and (b) specific surface area $S_r$, and for the extracted CNTs: (c) carbon content $C_e$ and (d) Specific surface area, $S_e$.

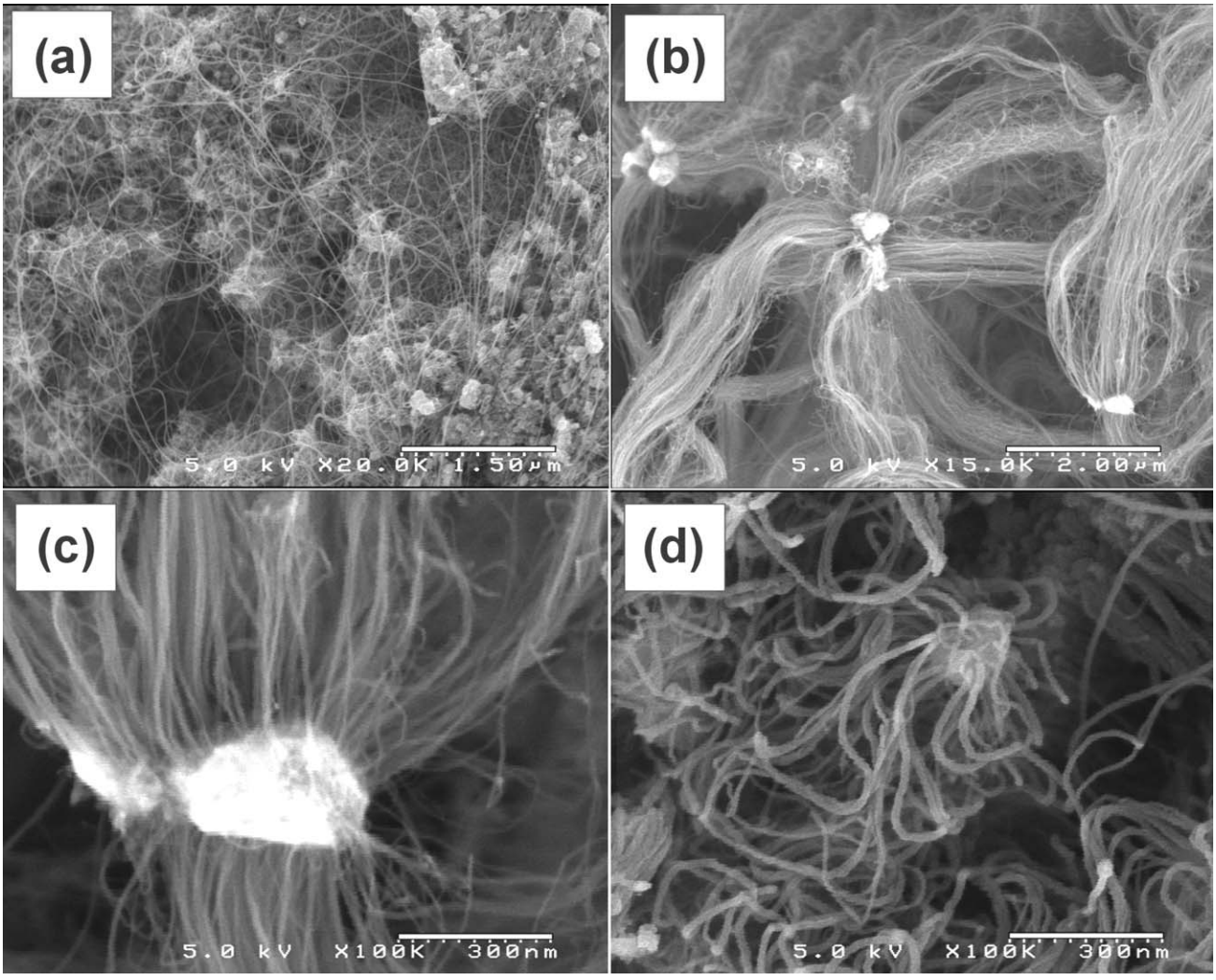


**Fig. 3** FEG-SEM images of CNT-containing composite powders for different molybdenum ratios: (a) $x = 0.25$; (b) $x = 0.67$; (c) $x = 0.67$ (higher magnification); (d) $x = 0.75$.

the CNTs is very clear and no sample from $x = 0.50$ exhibited any RBM signal at all. This indicates that the presence of CNTs with a diameter less than 2 nm is very unlikely in these samples.

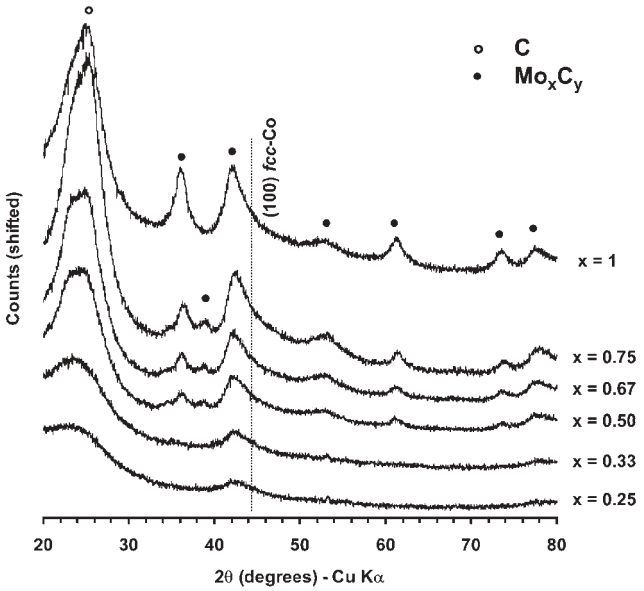


**Fig. 4** XRD pattern of the extracted CNTs. Only the carbon (002) peak and peaks from molybdenum carbides could be detected. The position of the (100) peak for fcc-Co is also shown.

The RBM peaks observed for $x = 0.25$ would correspond to diameters ranging from 1.04 to 2.5 nm (or 1.07 to 2.65 nm) if the CNTs are considered to be isolated or gathered into bundles (respectively).[8] The Raman process is influenced by optical resonance and this is especially true for CNTs. It is thus not possible with only one wavelength to scan the whole population of CNTs present within a sample, because a specific excitation wavelength enhances the signal for only some of the CNTs; moreover, RBM peaks cannot be observed for too low wavenumbers and this limits the observation range to a maximum diameter of about 3 nm. However, the samples showing RBM signals ($x = 0.25$ and 0.33) have some peaks in common (Fig. 5(a)), in particular at about 134 and 223 $cm^{-1}$. The corresponding diameters are 1.67 nm (1.82 nm for CNTs in bundles) and 1.00 nm (1.07 nm for CNTs in bundles), respectively. The difference in diameter is close to 0.7 nm and this indicates that these pairs of peaks could correspond to the outer and inner (respectively) diameter of DWNTs. For $x = 0.25$, another similar pair could be found between 114 and 176 $cm^{-1}$ (The corresponding diameters are 1.96 nm (2.16 nm for bundles) and 1.27 nm (1.37 nm for bundles), respectively).

Typical TEM images of the extracted CNTs are shown in Fig. 7. For $x = 0.25$, the CNTs are mainly individual, or gathered into thin bundles (no more than 20 nm in diameter), and no metal particles are visible (Fig. 7(a)). The diameter distribution of the CNTs is very uniform. For $x = 0.33$, some metal particles are occasionally found at the tips of the CNTs.

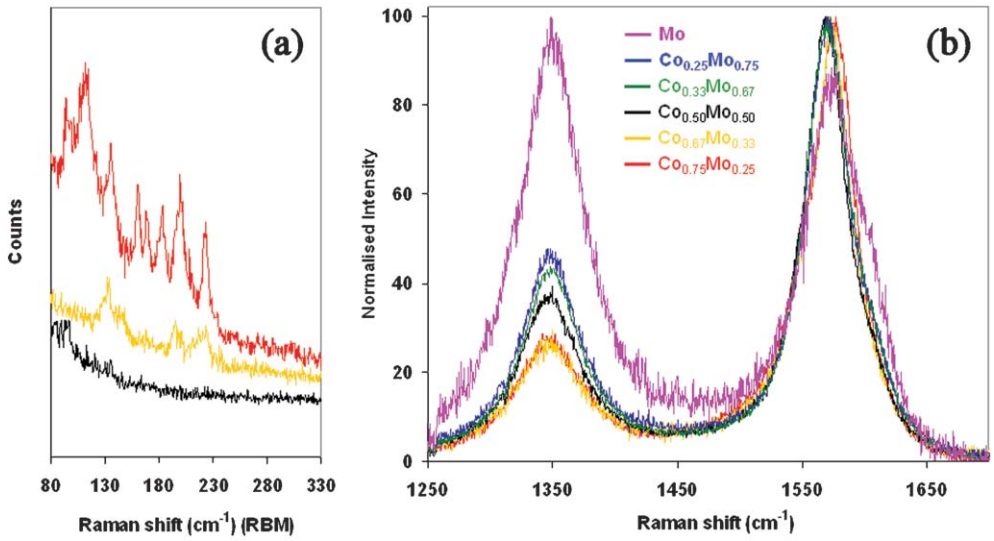


**Fig. 5** Raman spectra of the extracted CNTs: (a) RBM range (top: $x = 0.25$, middle: $x = 0.33$, bottom: $x = 0.50$), (b) high-frequency range: D and G bands.

The CNTs look slightly thicker but are still rather individual or forming thin bundles (Fig. 7(b)). From $x = 0.50$, some bamboo-like CNTs are present in the samples (Fig. 7(c)) and the number of walls of the CNTs obviously increases. The morphology of the sample is very different and the CNTs are forming threads looking like hair locks (Fig. 3(b)). It seems that the diameter distribution of the CNTs is less uniform and that large CNTs (around 15 nm diameter) are coexisting with thinner ones (around 1 nm diameter). Some of the largest CNTs exhibit obvious structural defects (wavy walls), but some still have straight walls. For $x = 0.67$ (Fig. 7(e)), a similar behaviour is observed, but the dispersion of the diameters is more marked. A metal particle is visible at the tip of some of the CNTs (Fig. 7(f)). The diameter of the metal particles typically ranges from 2.5 to up to 50 nm (Fig. 7(f)). The largest metal particles, found at the tip of large MWNTs, are often faceted (Fig. 7(f)) while the smallest ones are more spherical. The presence of metal particles at the tip of the CNTs becomes more and more frequent with the increase in the proportion of molybdenum. No obvious difference is found between $x = 0.67$ and 0.75, although some amorphous carbon deposit is clearly present in the latter. It also seems that the threads are shorter for $x = 0.75$. For $x = 1$, an important amount of poorly organised carbon is found in the sample, either covering the CNTs or forming large lumps. Most of the tubes show disorganised walls and numerous internal compartments.

HRTEM observation of the extracted samples confirms the Raman data. The only sample containing some SWNTs is for $x = 0.25$ but the number of observed SWNTs is very low. The CNTs are mainly DWNTs and triple-walled CNTs (TWNTs), representing together more than 93% of the population of CNTs (51% DWNTs, 42% TWNTs and 6% CNTs with four walls, Fig. 8(a)). The number of walls and diameters of the CNTs are obtained from the HRTEM images. The mean inner diameter is 1.7 nm (inner diameter ranging from 0.4 to 3.0 nm) and the mean outer diameter is 2.7 nm (outer diameter ranging from 1.1 to 4.6 nm). These data are in reasonable agreement with the diameters calculated from the Raman spectroscopy data (frequency of the RBM peaks). A similar HRTEM study for $x = 0.67$ (Fig. 8(c), (d)) indicated that the number of walls of the CNTs present in the sample is ranging from 2 to 13 (Fig. 8(c)), TWNTs being the main species and representing 22% of the whole population of CNTs. The mean inner diameter is 2.9 nm (inner diameter ranging from 0.8 to 3.9 nm) and the mean outer diameter 6.1 nm (outer diameter ranging from 3 to 12 nm or even more). A few MWNTs with an inner diameter as large as 8.5 nm are observed. Most of these CNTs present important structural defects (uncompleted walls, bamboo-like structure, and variation of the diameter along the length of the CNTs).

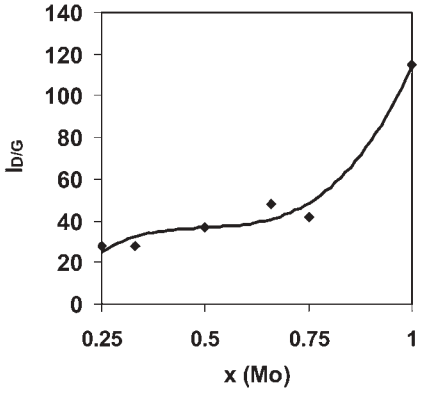


**Fig. 6** Variation of the intensity ratio between the D band and the G band ($I_{D/G}$) of the extracted CNTs with the molybdenum ratio in the corresponding starting oxides.

## Discussion

No SWNTs could be observed in any sample for $x > 0.25$, although the Raman data revealed the presence of RBM peaks for $x = 0.33$ as well; this means either that a very small amount of SWNTs are present for $x = 0.33$, or that these peaks arise from the presence of DWNTs (or even from CNTs with more than two walls). The increase in the number of walls of the CNTs, together with the observation of more and more structural defects, is in good agreement with the Raman data which indicated a continuous increase in the $I_{D/G}$ ratio with the increase in the molybdenum ratio. For $x = 1$, Raman spectroscopy even revealed that $I_{D/G}$ was $> 1$, indicating a high degree of disorder. This can also be correlated with the TEM observations which have shown a large amount of disordered and amorphous carbon in this sample. This may explain as well the slight increase in the specific surface area of the CNTs samples which was observed between $x = 0.67$ and 1, which could be attributed to some extent to the growing proportion of poorly organised carbon. Because the specific surface area of the starting oxides is rather low (values randomly scattered between 8 and 19 $m^2 g^{-1}$) and the variation of $S_r$ with $x$(Mo) is important, the surface increase (difference

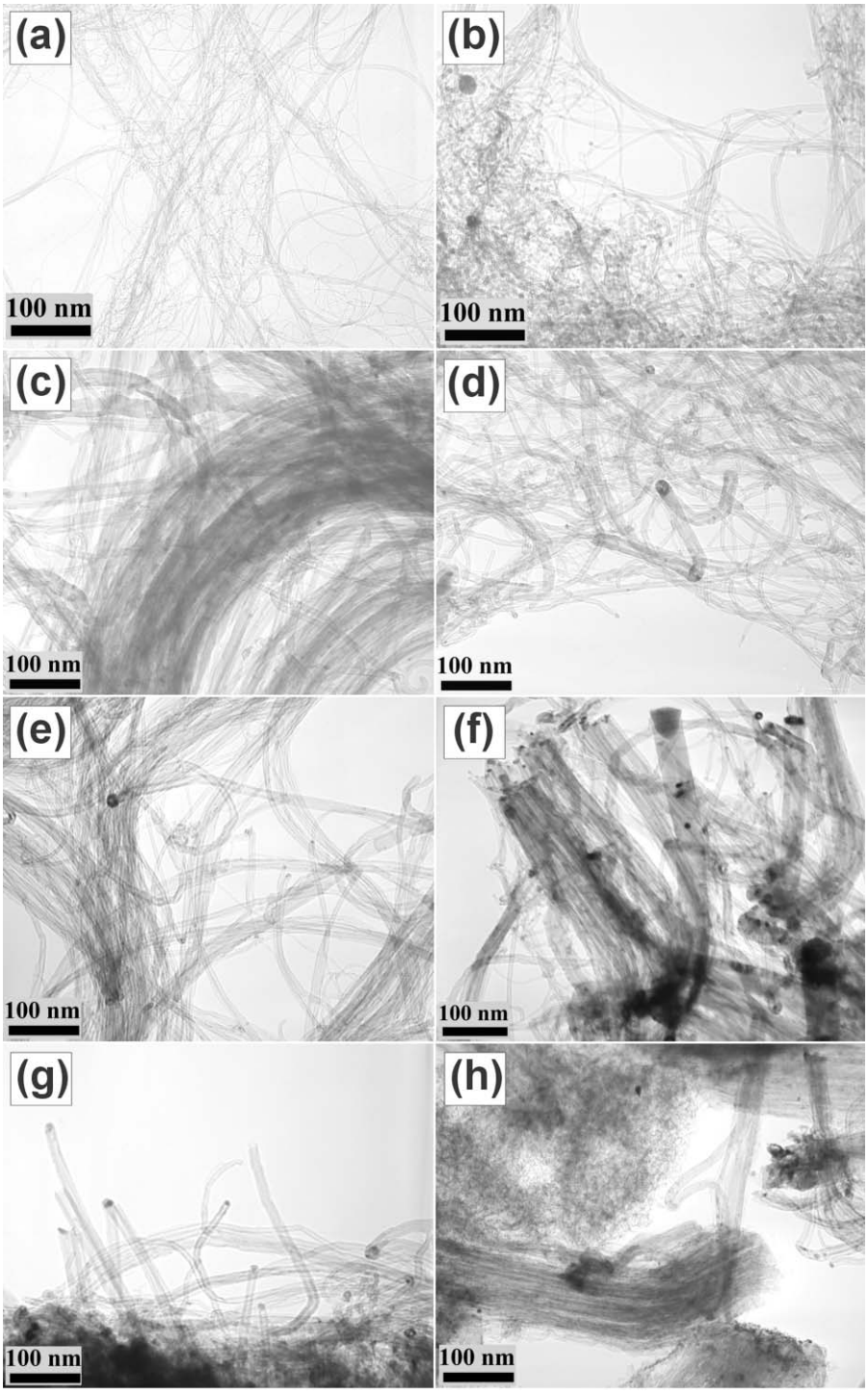


**Fig. 7** TEM images of extracted CNTs for different molybdenum ratios in the starting oxide: (a) $x = 0.25$, (b) $x = 0.33$, (c, d) $x = 0.50$, (e, f) $x = 0.67$, (g) $x = 0.75$, (h) $x = 1.00$.

between $S_r$ and $S_{so}$) is proportional to the surface of the whole population of carbon species present in the samples. Increasing values of $S_r$ indicate that the amount of CNTs is greater in the composite powders. This is nicely correlated to the variation of $C_n$, and that of the relative intensity of the (002) peak of graphitic material in the CNT-containing composite powders, which both follow exactly the same trend: a continuous increase up to $x = 0.75$, followed by a decrease for pure molybdenum. Because both $S_r$ and $C_n$ decrease together, this could be attributed to a lower catalytic activity for pure molybdenum compared to the mixtures of Co and Mo. The almost continuous decrease of $S_e$ (apart from the very last composition, for $x = 1$) could be explained by the TEM observations. Both the increase in the number of walls and the progressive increase in the proportion of metal particles at the tip of the CNTs contribute to the strong decrease of $S_e$.[7]

As a general trend, the increase in the ratio of molybdenum leads to a higher number of walls, together with an increase in both the inner and outer diameter. This was associated with a severe loss of selectivity towards the number of walls, as well as an important increase in the yield. This is in good agreement with the results of by Tang *et al.*,[3] who reported similar observations (although the total metal loading–Co and Mo–was not always kept constant, which made the comparison difficult). The formation of threads, looking like hair locks, seems to be typical of the presence of molybdenum over a given ratio ($x = 0.50$ in this study). This loss of selectivity towards SWNTs is however in apparent contradiction with the

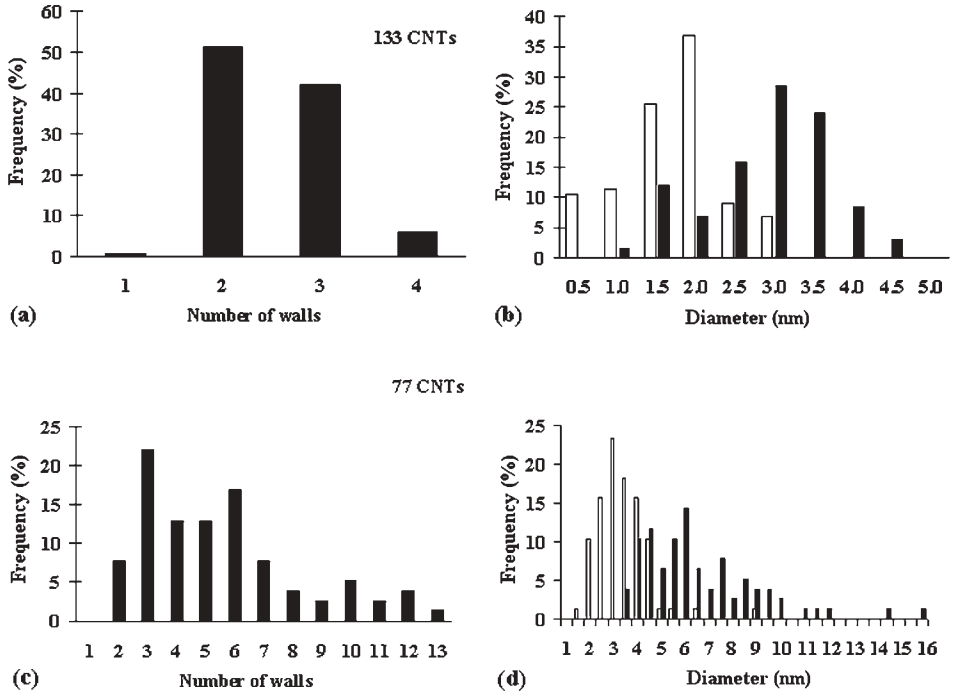


**Fig. 8** (a) Distribution of the numbers of walls and (b) distribution of inner ($d_i$) (white bars) and outer ($d_o$) diameter (black bars) for $x = 0.25$; $d_i$ (av.) = 1.7 nm, $d_o$ (av.) = 2.7 nm. (c) Distribution of the numbers of walls and (d) distribution of inner ($d_i$) (white bars) and outer ($d_o$) diameter (black bars) for $x = 0.67$; $d_i$ (av.) = 2.9 nm, $d_o$ (av.) = 6.1 nm.

observations of Resasco's group,[2,9] obtained using the same metals (Co and Mo) but with CO as the carbon source. They first reported an increase in the selectivity towards SWNTs by adding Mo to Co, which we do not confirm in this work with $CH_4$, even with the lowest proportion of molybdenum ($x = 0.25$). They also reported that the use of molybdenum alone did not lead to any CNT, as opposed to results reported by Dai *et al.*[1] who prepared SWNTs from CO using pure molybdenum as the catalyst. The main differences with our work are (1) the use of $CH_4$ instead of CO, the reactivity of which is different and also implies to work at a higher temperature and (2) the preparation of the catalyst, which also plays a very important role (different specific surface area, crystallographic form, *etc.*[10]). Alvarez *et al.*[9] reported that on the one hand when the ratio of molybdenum is low, the formation of the oxide $Co_3O_4$ is favoured; on the other, when the ratio of molybdenum is high, $CoMoO_4$ is formed. The catalysts used in Resasco's reports were all prepared by impregnation of commercial $SiO_2$ powder (480 $m^2\ g^{-1}$) by aqueous solutions of Co(II) and Mo(VI) salts. This is an important difference with our process, in which Co(II) ions are known to be in solid solution in MgO. For this reason, they are more difficult to reduce than Co(II) ions dispersed at the surface of $SiO_2$ grains. The acidity of $SiO_2$ compared to the basicity of MgO may also play a role in the catalytic properties of the starting oxides. In our case, because Mo ions are not in solid solution, we suppose that increasing the molybdenum ratio will lower the homogeneity of their distribution in the starting oxide, which will in turn result in more and more heterogeneous local Mo:Co ratios and thus the diameter distribution of the CNTs must be larger and larger, as observed by TEM. It seems that CNTs with a small diameter are always present in the samples (although their proportion tends to decrease when $x$ increases) but that the proportion of CNTs with larger diameters increases with $x$(Mo). Herrera *et al.*[11] indicated that small Co clusters (formed by delayed reduction of $CoMoO_4$) would be at the origin of SWNTs, when larger Co particles would generate MWNTs, in agreement with our previous work. They found $Mo_2C$ in the samples after the CCVD step, similarly to this work, but only when Co was associated to molybdenum, which is different from this work where molybdenum carbides are systematically detected by XRD, even in the absence of cobalt ($x = 1$). If the synergistic effect of mixing Co and Mo is once more confirmed by the present work, the mechanisms involved are different. In this study, molybdenum is unlikely to delay the reduction of Co(II) ions and to favour the formation of smaller Co nanoparticles. Mo ions, which may be present in the form of different $MoO_x$ oxides in the starting oxides, must be reduced by the $H_2$–$CH_4$ mixture to form different molybdenum carbides. Molybdenum is known to be a promoter for the aromatisation of $CH_4$ but the real nature of the catalytic molybdenum compound is still unclear in our case ($MoO_x$, $Mo_xC_y$?). This is probably the reason why a small ratio of molybdenum significantly enhances the formation of CNTs, by providing the Co nanoparticles with very active carbon species; introducing too much molybdenum however increases too much the activity of the catalyst and probably provides the Co nanoparticles too fast with carbon which would be likely to favour the formation of MWNTs with many structural defects, as observed experimentally. It is likely that the metal particles found at the tip of most of the CNTs when $x \geqslant 0.67$ are made of molybdenum carbide, as no cobalt could be detected clearly in the extracted CNTs. This may indicate that increasing the molybdenum ratio (and thus decreasing the available amount of Co) provoked the formation of MWNTs on metal particles coming from a molybdenum precursor, in addition to the other CNTs forming on the Co nanoparticles.

It is also interesting to compare the results obtained in this work for $x = 0.25$ with what was obtained using the same composition of the starting oxide in identical CCVD conditions, but with a different preparation[12] (replacing the urea by citric acid during the combustion process); Working with citric acid allowed milder combustion conditions and led to a higher specific surface area of the starting oxide. Our previous report using this catalyst[12] indicated that the CNTs were mainly DWNTs (77%) and that no CNT with more than three walls could be found. It thus seems that any difference in

the preparation of the oxide catalyst can lead to drastic modifications of the number of walls of the CNTs, allowing some control of this parameter. This must also be compared with the results reported by Tang *et al.*[3] who reported very different results than our previous work,[13] working with the same $Mg_{0.95}Co_{0.05}O$ solid solution (prepared by a different route), exactly in our CCVD experimental conditions. They obtained low quality CNTs (Raman $I_{D/G}$ close to 120%, which was explained by the presence of amorphous carbon in the sample), and did not comment the number of walls. However, our results presented good quality SWNTs and DWNTs (almost 90% of the CNTs), without amorphous carbon deposit (Raman $I_{D/G}$ close to only 20%). More work is in progress to study the influence of the starting oxide preparation conditions and to determine the activity of starting oxides with $x(Mo) < 0.25$.

## Conclusion

$Mg_{0.99}(Co_{1-x}Mo_x)_{0.01}O$ (with $x = 0.25, 0.33, 0.5, 0.67$ and 1.0) oxides prepared by ureic combustion were reduced in $H_2$–$CH_4$ atmosphere in order to form CNT-containing composite powders. The MgO matrix and most of the residual (Co, Mo) catalyst are easily dissolved by a HCl soaking, leading to CNTs samples with a high purity (up to 98.6 at% of carbon). The variation of the ratio between cobalt and molybdenum was found to modify both the yield in CNTs and their basic characteristics (number of walls, diameter distribution). Increasing the molybdenum proportion until $x \leqslant 0.67$ leads to an increase in the yield in CNTs. However, this also leads to an increase in the number of walls of the CNTs, together with a growing proportion of CNTs with a large amount of structural defects (bamboo-like structures) as well as the presence of some deposits of poorly-organised carbon. CNTs prepared with the starting oxide containing only molybdenum were all containing numerous structural defects and covered with some carbon deposit. Although the exact nature of the molybdenum species at the various stages of the process is still unclear, as are some possible cobalt–molybdenum interactions, it is proposed that a small ratio of molybdenum significantly enhances the formation of CNTs, by providing the Co nanoparticles with very active carbon species coming from the aromatisation of $CH_4$ by molybdenum. However, introducing too much molybdenum probably provides the Co nanoparticles too rapidly with carbon, which is likely to favour the formation of MWNTs with many structural defects.

Fine tuning the key synthesis parameters such as the ratio between cobalt and molybdenum and the total amount of these elements in the starting oxide, the reduction temperature and the atmosphere composition, will allow a better control on the number of walls. The CNTs prepared with the lowest proportion of molybdenum ($x(Mo) = 0.25$) were mainly double- and triple-walled CNTs, with a specific surface area of 800 $m^2\,g^{-1}$, a carbon content of 92.4 wt% (98.3 at%) and a yield close to 10 wt% with respect to the starting oxide.

## Acknowledgements

We acknowledge Lucien Datas from the Service Commun de Microscopie à Transmission for his help with TEM and HRTEM observations and the Groupement Interuniversitaire de Spectroscopie Raman (both at University Paul Sabatier) for the Raman spectroscopy.

## References

1 H. Dai, A. G. Rinzler, P. Nikolaev, A. Thess, D. T. Colbert and R. E. Smalley, *Chem. Phys. Lett.*, 1996, **260**, 471–475.
2 B. Kitiyanan, W. E. Alvarez, J. H. Harwell and D. E. Resasco, *Chem. Phys. Lett.*, 2000, **317**, 497–503.
3 S. Tang, Z. Zhong, Z. Xiong, L. Sun, L. Liu, J. Lin, Z. X. Shen and K. L. Tan, *Chem. Phys. Lett.*, 2001, **350**, 19–26.
4 K. C. Patil, *Bull. Mater. Sci.*, 1993, **16**, 533–541.
5 E. Flahaut, A. Peigney, Ch. Laurent and A. Rousset, *J. Mater. Chem.*, 2000, **10**, 249–252.
6 A. Peigney, Ch. Laurent, F. Dobigeon and A. Rousset, *J. Mater. Res.*, 1997, **12**, 613–615.
7 A. Peigney, Ch. Laurent, E. Flahaut, R. Bacsa and A. Rousset, *Carbon*, 2000, **39**, 507–514.
8 L. Alvarez, A. Righi, T. Guillard, S. Rols, E. Anglaret, D. Laplaze and J. L. Sauvajol, *Chem. Phys. Lett.*, 2000, **316**, 186–190.
9 W. E. Alvarez, B. Kitiyanan, A. Borgna and D. E. Resasco, *Carbon*, 2001, **39**, 547–558.
10 Ch. Laurent, A. Peigney and A. Rousset, *J. Mater. Chem.*, 1998, **8**, 1263–1272.
11 J. E. Herrera, L. Balzano, A. Borgna, W. E. Alvarez and D. E. Resasco, *J. Catal.*, 2001, **204**, 129–145.
12 E. Flahaut, R. Bacsa, A. Peigney and Ch. Laurent, *Chem. Commun.*, 2003, 1442–1443.
13 R. R. Bacsa, Ch. Laurent, A. Peigney, W. S. Bacsa, Th. Vaugien and A. Rousset, *Chem. Phys. Lett.*, 2000, **323**, 566–571.